Geologic Map of the Cerbat 7 ½' Quadrangle, Mohave County, Arizona

by

Carson A. Richardson and Philip A. Pearthree

Arizona Geological Survey
Digital Geologic Map 151

January 2022

Arizona Geological Survey
University of Arizona
1955 East Sixth Street, Suite 205, Tucson, Arizona 85721

Includes 20 pages text and one 1:24,000 scale geologic map

This geologic report was funded in part by the USGS National Cooperative Geologic Mapping Program under STATEMAP award number G19AC00381, 2019. The views and conclusions obtained in this document are those of the authors and should not be interpreted as necessarily representing the official policies, either expressed or implied, of the U.S. Government.

LOCATION AND ACKNOWLEDGEMENTS

The study area includes the southern Cerbat Mountains and a portion of northern Sacramento Valley in Mohave County, northwest Arizona (Fig. 1). Elevations vary across the study area, with elevations in Sacremento Valley ranging from 2900' in the southwest to 3800' in the northeast, and the Cerbat Mountains start at 3600' to 3800' along the western margin, with major peaks ranging from 5100' to 6230'. The area lies within the Mohave Desert with large areas of relatively open desert in Sacramento Valley punctuated by thick brush zones along major washes. Bedrock geology was mapped by Carson Richardson during the spring of 2020, and the surficial geology was mapped by Philip Pearthree in the spring of 2020. Some areas within the vicinity of the Mineral Park mine and patented mining claims were mapped using remote techniques and compilation of previous published mapping and reports.

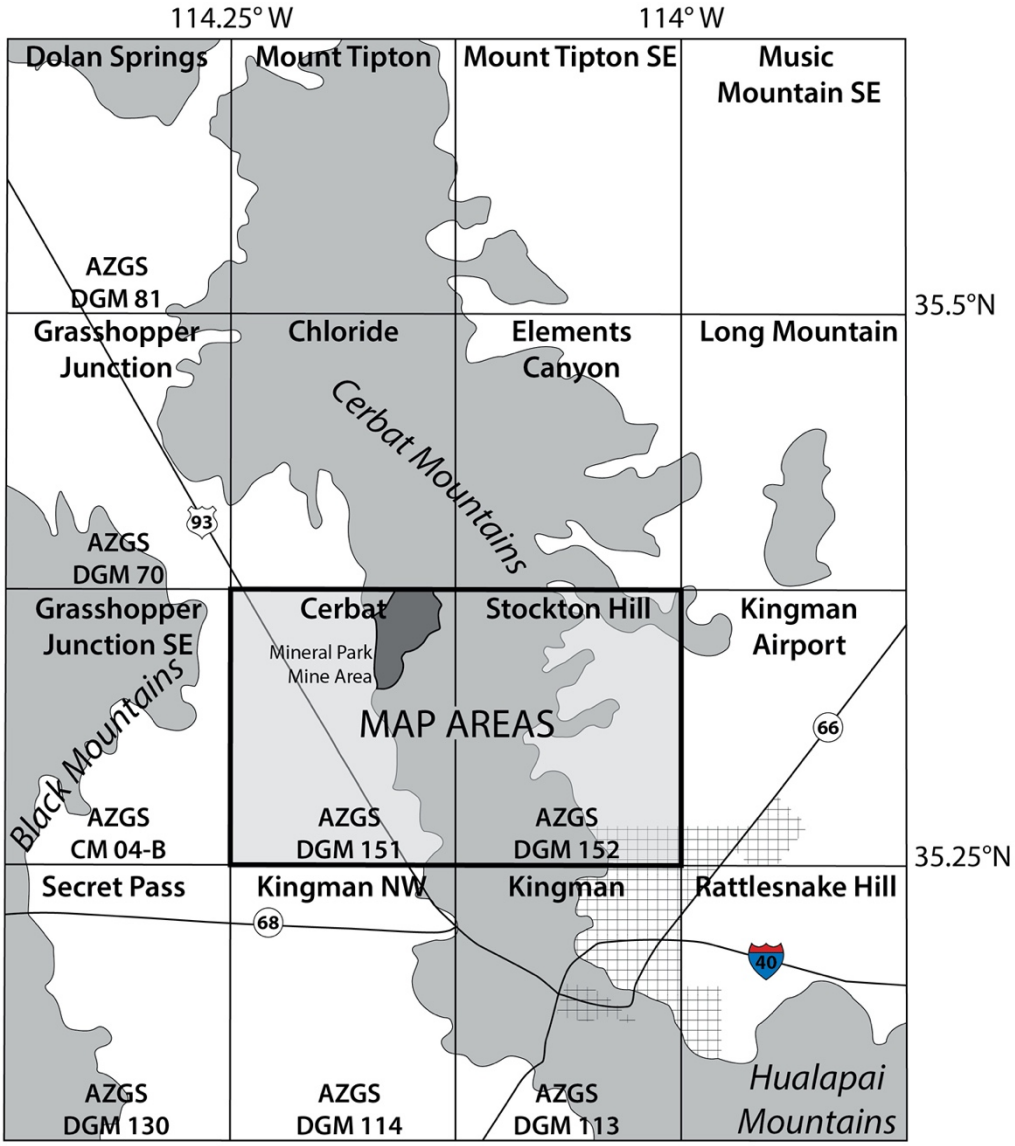

Figure 1. *Regional geography and USGS 7.5' quadrangles in the vicinity of the map area.*

Mapping was supported by the United States Geological Survey and the Arizona Geological Survey as part of the National Cooperative Geologic Mapping Program, under USGS award number G19AC00381. We wish to acknowledge discussions with William Wilkinson and Roy Greig.

PREVIOUS STUDIES

Geologic investigations of the Cerbat Mountains and its mining districts have been conducted for over a century, starting with several initial reconnaissance-scale studies (Lee, 1908; Schrader, 1909). The first focused study of the geology of the southern Cerbat Mountains was by Thomas (1949a, 1949b, and 1953). Dings (1951) provided a comprehensive study of the ore deposits and produced the first 1:24,000-scale geologic map of the area. Much of the research from the 1960's to 1980's was by economic geologists examining on the porphyry molybdenum-copper mineralization at Mineral Park and/or porphyry-related vein deposits throughout the district (Eidel et al., 1968; Drake, 1972; Laine, 1974; D'Andrea et al., 1977; Eaton, 1980; Wilkinson, 1981; Wilkinson et al., 1982; Vega, 1984; Lang, 1986; Lang and Eastoe, 1988; Lang et al., 1989). The Cerbat Mountains was one of the field sites studied by Palais (1991) for his Ph.D. dissertation on low-pressure metamorphism. Ernie Duebendorfer and his students at Northern Arizona University conducted numerous detailed studies throughout the northern and central Cerbat Mountains (Hanlon, 1997; Orr, 1997; Jones, 1998; Duebendorfer et al., 2001). Known work, but currently inaccessible due the lack of accessible digital copies, also includes that of several German graduate students who conducted work in the Cerbat Mountains on aspects ranging from Proterozoic structure to the geochemistry of Tertiary volcanic rocks (Mötz, 1996a, 1996b; Donner, 1997; Schneider, 1997; Henrik, 1998; Kollet, 1998).

SURFICIAL DEPOSITS

Surficial deposits of the map record the recent geologic history of this area. The western piedmont of the Cerbat Mountains in the map drains to the southwest in Sacramento Valley, and then to the south to the Colorado River. Lack of any evidence for long-term incision in the axis of Sacramento Valley indicates that regional base level for the fluvial systems draining the map area has been fairly stable through the Quaternary. Given this stable base level, Quaternary alluvial fan and terrace deposits probably record periods of piedmont aggradation and incision driven by climate changes that altered the quantity of sediment supplied from the mountains and the ability of tributary fluvial systems to transport that sediment (e.g., Bull, 1991).

The piedmont in the map area is covered primarily by late to middle Pleistocene alluvial fan deposits (map units Qi3, Qi2, Qi1, and Qi), with older Pleistocene deposits (unit QTa) preserved in a few limited upper piedmont areas. Holocene alluvial fan, terrace, and wash deposits are extensive in some areas. These deposits typically have modest topographic relief, and much of these areas may be prone to inundation in large flood events.

None of the Quaternary units are directly dated, but in the lower Colorado River Valley Qi3 deposits were graded to the maximum Colorado River aggradation recorded by the Chemehuevi Formation, 50-100 ka (Malmon et al., 2011).

STRUCTURAL GEOLOGY

The structural geology of the Cerbat Mountains records at least three, and possibly four or more, distinct tectonic episodes in the Paleoproterozoic, Eocene(?), and Miocene (or later).

Paleoproterozoic

Early workers in the Cerbat Mountains documented evidence of folding within the crystalline rocks from regional-scale map patterns of the amphibolites and metamorphic rocks along the western flanks of the Cerbat Mountains, with three major antiforms defined from the town of Chloride to Cerbat Canyon (Thomas, 1953; Wilkinson et al., 1982, Fig. 26.4; Fig. 2). Wilkinson et al. (1982) describes two major domains of Precambrian foliation: 1) an earlier domain along the western Cerbat Mountains of more variable foliation concordant with lithologic layering that defined the steep, open synforms and antiforms, and 2) a later domain of steeply dipping northeast to east-northeast-striking foliation in the eastern Cerbat Mountains. Eaton (1980, Fig. 28), working in the Chloride mining district north of Mineral Park, suggested that large antiform first documented there by Thomas (1953) could be a composite feature representing three generations of Precambrian folds.

Duebendorfer et al. (2001) was the first published study in the Cerbat Mountains to look exclusively at the Paleoproterozoic deformation and documented two events. The first event (D_1), best preserved in the northern Cerbat Mountains, is characterized by a north-northwest-striking, moderately northeast dipping foliation that is axial planar to macroscopic, west-southwest-vergent, recumbent folds and is bracketed between 1740-1721 Ma (Orr, 1997; Duebendorfer et al., 2001). The second Paleoproterozoic event (D_2) is represented by a northeast-striking subvertical foliation that transposes the earlier foliation, is the dominant fabric in the central and southern Cerbat Mountains, and is bracketed between 1724-1680 Ma (Jones, 1998; Duebendorfer et al., 2001). Where both fabrics are known or thought to be present, Duebendorfer et al. (2001) describe D_1 fabrics as generally truncated or transposed into parallelism by D_2 fabrics. Folds associated with D_2 have moderate to steep plunges to the north and northeast (Duebendorfer et al., 2001). Hanlon (1997) suggests that the northwest-striking D1 fabrics were transposed into moderately northeast-plunging isoclinal folds. Metamorphism associated with each deformation event contains mineral assemblages indicating metamorphism to granulite facies (Palais, 1991; Duebendorfer et al., 2001).

This study found the northeast-striking subvertical foliation to be dominant fabric through the southern half of the map (principally south of Cerbat Canyon and following the Xu-Xgn contact to the eastern quadrangle boundary). North of this area, the orientation of foliation is more variable, but generally is subparallel to lithologic layering as described by Wilkinson et al. (1982). The antiform north of Cerbat Canyon and southwest of Mineral Park plunges ~47°NNW, but is not isoclinal (Fig. 2; map sheet). Additionally, this area lacks strongly developed northeast-striking, subvertical D_1 foliation which has been suggested to be the cause of the north to northeast-plunging folds. The folding north of Cerbat Canyon, first documented Thomas (1953) and Wilkinson et al. (1982), is interpreted here as comparable to the D_1 event of Duebendorfer et al. (2001) with a greater diversity of orientations and structural styles for D_1 events.

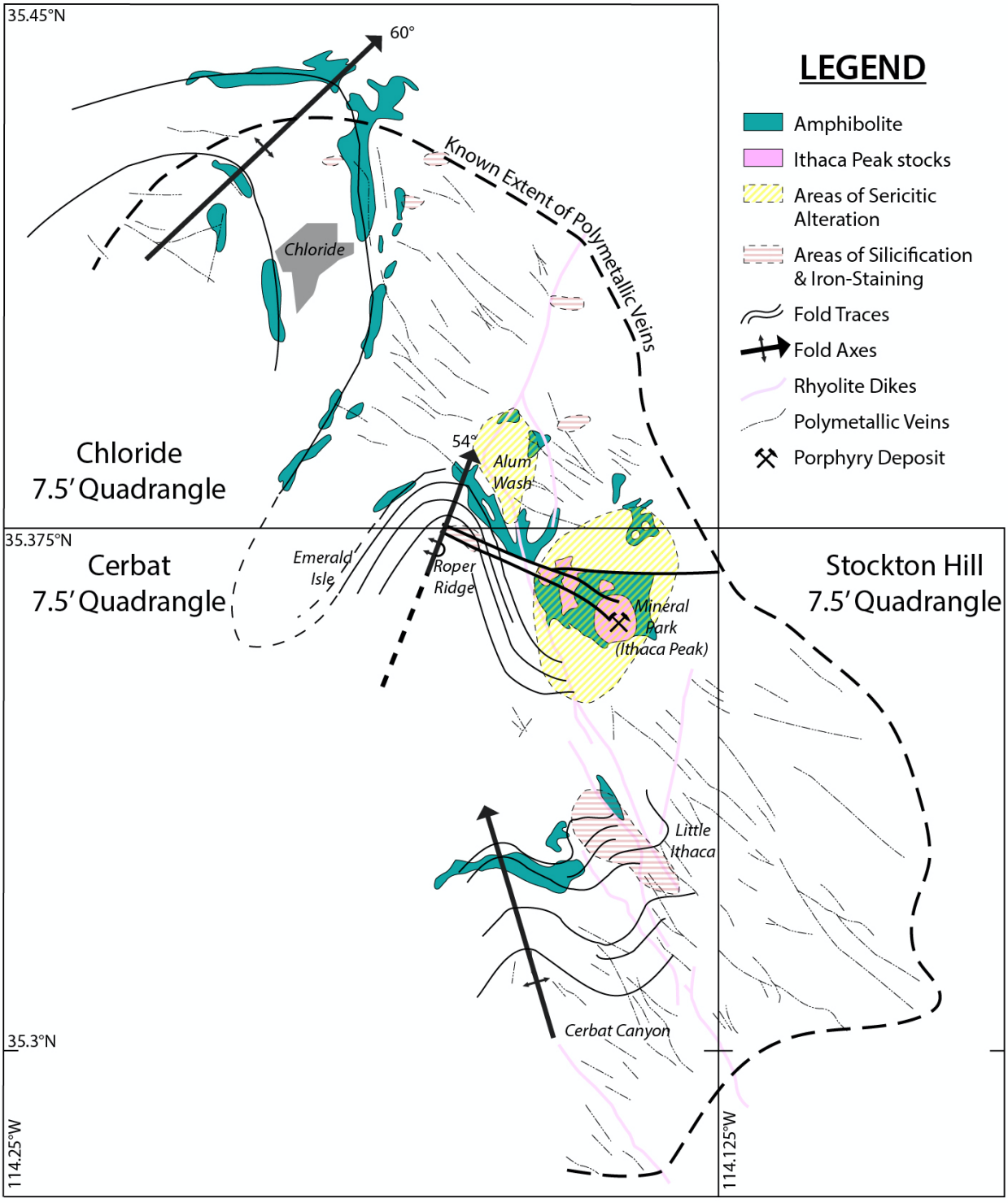

Figure 2. *Generalized map of the Wallapai district (adapted from Wilkinson et al., 1982 and Vega, 1984).*

Eocene: Potential Laramide structure / thermochronologic results

Regionally, Paleozoic and Mesozoic stratified rocks are absent throughout northwest Arizona, with Cenozoic volcanic and sedimentary rocks directly overlying Proterozoic and Cretaceous crystalline rocks (Richard et al., 2000). This missing stratigraphy has been attributed to the Kingman uplift, a hypothesized Laramide reverse fault and regional uplift (Lucchitta, 1975; Young, 1979). The causative fault has not been identified, but Faulds et al. (2001) and Beard and Faulds (2011) suggest that the reverse fault could be buried in Sacramento Valley. This is based on the juxtaposition of two-mica, garnet-bearing, strongly peraluminous Cretaceous plutons in the Black Mountains (considered to be the hanging-wall block) that would have been emplaced at depths of at least 10 km based on their phase relations (Faulds et al., 2001) compared to the footwall block with shallowly emplaced plutons such as Clay Springs or Ithaca Park (Young, 2001). The Ithaca Peak stocks were emplaced at depths 3±1 km based on fluid inclusion data and stratigraphic reconstructions (Wilkinson et al., 1982; Lang and Eastoe, 1988). North of the Cerbat Mountains in the White Hills, Fitzgerald et al. (2009) used apatite fission track thermochronology to document cooling between ~70-50 Ma that predates any extensional events and is interpreted to be related to Laramide tectonic exhumation.

To test this hypothesis, we determined to conduct apatite (U-Th)/He thermochronology on Laramide porphyritic rocks in the Cerbat Mountains to avoid any partially reset pre-Laramide thermal signatures. Apatite (U-Th)/He thermochronology documents rock cooling below ~80-40°C or ~4-2 km paleodepths (Murray et al., 2018). Apatite grains from the Mineral Park biotite quartz monzonite porphyry (map unit Kbqp) were obtained from mineral separates provided by Roy Greig from his recent U-Pb zircon geochronologic efforts. Samples were analyzed at the Arizona Radiogenic Helium Data Laboratory at the University of Arizona in Tucson, Arizona. Averaged analytical results are given in Table 1, along other analytical results from work related to this mapping project. Individual grain cooling ages ranged from ~48-60 Ma. Thermal modeling of the Cerbat Mountains was conducted using HeFTy, with the following constraints: emplacement of Ithaca Peak stock between 73.2 ± 0.5 Ma at depths of 2-4 km, igneous cooling and Laramide orogenesis (either exhumation or burial) in the ~20 million year period that follows, and the Ithaca Peak stock must be near the surface between 15 Ma to present to allow for the weathering of hypogene copper to form the Emerald Isle exotic copper deposit. Results from the best-fit path from the Monte Carlo simulation in HeFTy suggest that the Cerbat Mountains experienced rapid exhumation ca. ~55 Ma and has been within a 1-2 km of the surface since then (Fig. 3). The cooling period could be related to exhumation within the hanging-wall block of a Laramide reverse fault or erosional exhumation.

Table 1. Geo/Thermochronologic Analytical Results

Sample	Latitude	Longitude	Method	Mineral	Age (Ma)	Error (Ma)	Laboratory
648	35.3591	-114.142	(U-Th)/He	Apatite	57	0.4	UAARHDL
648 (Greig, 2021)	"	"	U-Pb	Zircon	73.2	0.5	UA ALC
CAR-CB20-09	35.28373	-114.131	U-Pb	Zircon	1439	26	BS IGL
CAR-20CB-29	35.32983	-114.136	U-Pb	Zircon	74.5	0.7	UA ALC

Miocene to Present: Extensional Faulting

Regionally, extensional faulting was ongoing from ~18-13 Ma, waning from ~13-8 Ma, with relative tectonic quiescence since 8 Ma (Faulds et al., 1997, 2001). Extensional faulting is known to be nearby in the Black Mountains, the Grasshopper Junction area, Kingman area, and Hualapai Valley and commonly associated with variable amounts of tilting (Faulds et al., 1997; Varga, 2001; Ferguson et al., 2009; Ferguson and Cook, 2015). While the Cerbat quadrangle lacks stratified rocks of Cenozoic age, volcanic rocks in the Stockton Hill quadrangle record only gentle (generally less than 10° of eastward tilting), with the southern Cerbat Mountains looking only minimally faulted and tilted.

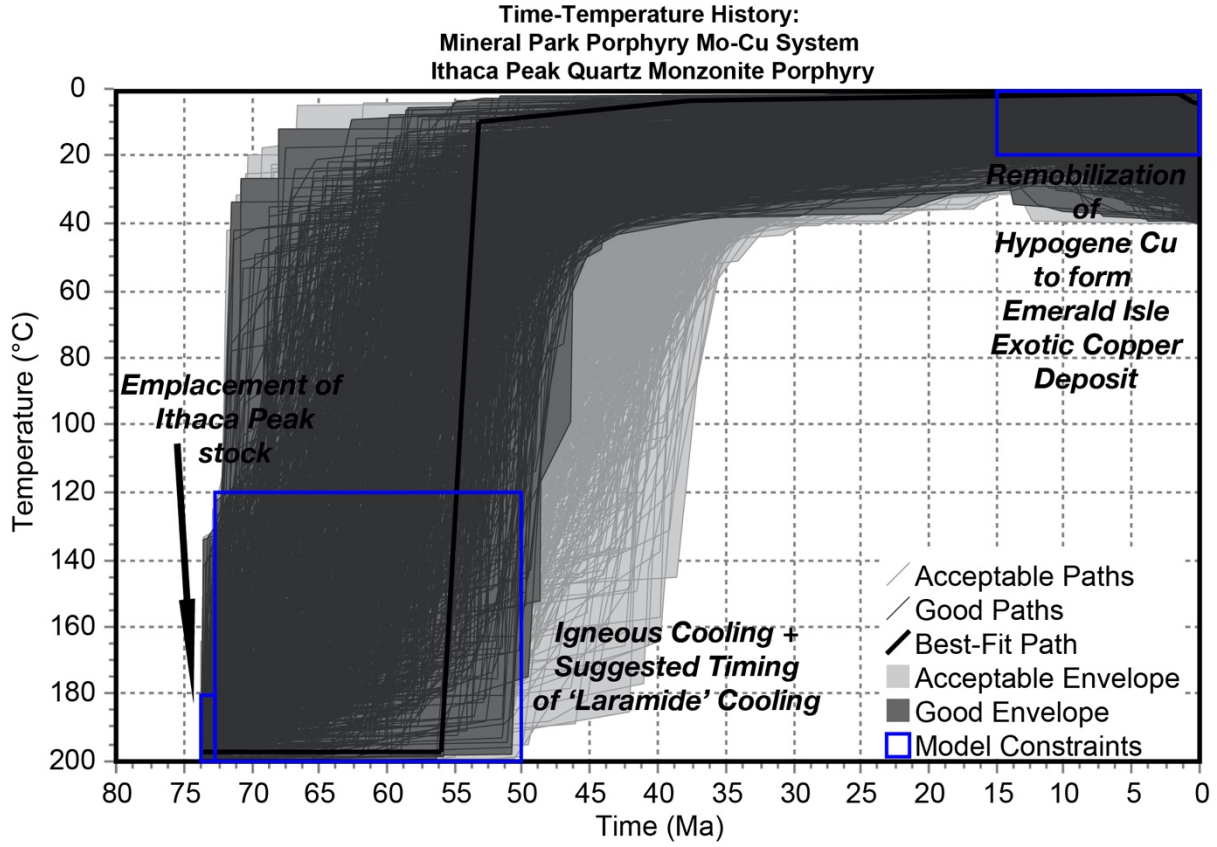

Figure 3. *Time-temperature history of the Ithaca Peak stock.*

The principal fault that past workers have discussed is the Sacramento fault. First described by Thomas (1953), the Sacramento fault is a SE-striking, high-angle, west-dipping normal fault bounding the western extent of the Cerbat Mountains. The fault was described based on: 1) the juxtaposition of volcanic rocks along the westernmost foothills older rock at higher elevations in the area of the Grasshopper Junction 7.5' quadrangle, and 2) the lack of outcropping exposures of older rocks west of the margin of the range. The Sacramento fault was interpreted to be responsible for the gentle tilting of volcanic rocks along the eastern edge of the range. Volcanic rocks along the eastern foothills of the Cerbat Mountains dip eastward and are interpreted to be the base of the Tertiary sequence of the Hualapai Valley (Faulds et al., 1997). Mapping of the Grasshopper Junction 7.5' quadrangle by Ferguson et al. (2009), documented the

volcanic rocks display a fanning sequence of southwesterly dips from ~60° to ~20°, and thus must have been dismembered and tilted by east-dipping normal faults and not a west-dipping normal fault. The only west-dipping normal fault is poorly exposed fault in the Emerald Isle pit that down-drops ~100-200 feet of slip (Agnerian and Postle, 2006).

MINERAL DEPOSITS

Mineralization in the southern Cerbat Mountains consists of four principal mineral deposit types: 1) porphyry molybdenum-copper, 2) porphyry-related polymetallic veins, 3) exotic copper, and 4) pegmatite-related REE (not described here as the principal occurrence, the Kingman Feldspar mine, is located on the Stockton Hill quadrangle).

Porphyry molybdenum-copper

Porphyry molybdenum-copper alteration and mineralization is documented in the Wallapai district at Mineral Park, Alum Wash, and Little Ithaca (Fig. 2). Potassic, sericitic, and argillic(?) alteration types are present at Alum Wash and Mineral Park, while only potassic alteration is observed at Little Ithaca.

Detailed descriptions of the porphyry-related alteration and mineralization can be found in Eidel et al. (1968), Wilkinson et al. (1982), and Vega (1984). In brief, the earliest alteration is pre-ore "selectively pervasive" partial to complete replacement of only certain minerals by biotite or K-feldspar. Other pre-ore alteration includes barren biotite and K-feldspar veinlets. Later major vein types include quartz + K-feldspar + biotite + anhydrite + pyrite + molybdenite veins, followed by quartz + molybdenite + pyrite veins, quartz + chalcopyrite + pyrite + chlorite ± magnetite + K-feldspar ± epidote ± anhydrite veins, and quartz + pyrite + sericite ± carbonate veins. The potassic alteration observed at the Little Ithaca area constitutes thin K-feldspar veinlets cutting granite gneiss with no major Cretaceous intrusive rocks exposed (Vega, 1984). The extent of major sericitic alteration is shown on Figure 2.

Vega (1984) also describes an additional alteration type termed J_2 fracture-alteration. J_2 fractures, originally named by Heidrick and Titley (1982), these fractures are discontinuous, curviplanar factures that form craggy iron-stained bleached ridges, with brecciated open-spaced filling found near center of zone. Eaton (1980) described similar silicified, iron-stained alteration zones near Chloride. These are shown in Figure 2 as "Zones of Silicification and Iron-Staining."

Wilkinson et al. (1982) concluded that the exposed Cretaceous rocks at the Mineral Park mine are not related to the porphyry mineralization, but must predate the mineralizing event based on the distribution of alteration and mineralization features, the narrow range of homogenization temperatures, and the lack of high homogenization temperatures that are typical of the near pluton environment. A deep drill hole (~1.5 km) in the middle of the mine did not encounter other intrusive rocks or different mineralization. Lang and Eastoe (1988, Fig. 1) outlined the inferred boundary of the causative intrusion based on peak temperatures >400°C from polymetallic quartz veins in the Wallapai district. The foci of porphyry mineralization at Mineral Park, and not at Alum Wash or Little Ithaca, is interpreted to be due to the fracturing associated with the emplacement of the Ithaca Peak stocks that later helped guide mineralizing ore fluids from depth (Wilkinson et al., 1982; Lang and Eastoe, 1988).

An elliptical zone, measuring 210 m x 150 m, of crenulated quartz veins and large quartz pods and masses with unidirectional solidification textures (USTs) occurs within the quartz porphyry (map unit Kqp) at Mineral Park (Eidel et al., 1968; Wilkinson et al., 1982, Fig. 26.1). USTs define mineral growth direction from a solid substrate and are found in many different magmatic-hydrothermal deposits (Shannon et al., 1982; Kirwin, 2006). USTs occur in apical portions of porphyry intrusions, with crystal growth inward from the roof and walls of a magma chamber. In porphyry molybdenum systems, dense UST zones define internal textural subdivisions between individual intrusions (Shannon et al., 1986; Seedorff et al., 2005). In porphyry copper systems, UST types can vary from monomineralic (such as the crenulated quartz layers at Mineral Park) to polymineralic layers including quartz, magnetite, and Cu-Fe-sulfides (Atkinson and Ware, 2002). In some deposits, it has been demonstrated that crenulate quartz layers are compositionally distinct from phenocryst/groundmass quartz and are interpreted to be hydrothermal in origin (Lowenstern and Sinclair, 1996). Thus, USTs are thought to record the transition between magmatic and hydrothermal conditions in the presence of aqueous fluids that have accumulated near the apex of a porphyry stock (Lowenstern and Sinclar, 1996; Seedorff et al., 2005). The presence of the crenulated quartz USTs in the quartz porphyry could be suggestive that the exposed Ithaca Peak intrusions focused aqueous fluids into the different stocks during their crystallization history and potentially produced a long-since eroded porphyry system that would have above the modern Mineral Park mining complex.

Porphyry-related polymetallic veins

The polymetallic vein deposits in the Wallapai district are zoned around the Mineral Park porphyry system, with an innermost copper-molybdenum core surrounded by a manganese halo, to a copper zone, intermediate lead-zinc zone, and an outer silver-gold zone with a variably overlapping zone of arsenic from the Pb-Zn to Ag-Au zones (Fig. 4; Eidel et al., 1986, Fig. 5; Lang and Eastoe, 1998, Fig. 4). The vein deposits range in width from a few inches to up to ~50 feet wide, but when larger than ~30 feet, the deposits are more accurately lodes or vein zones (Thomas, 1949). Vega and Wilkinson (1984) report that some historic vein widths were exaggerated as they included unmineralized wall rock between vein branches. Veins are planar to gently curving structures with steep dips (>60°) to the northeast and southwest, strike between N30°-50°W, have strike lengths from 30 m to 4 km, and crop out as iron-stained siliceous boxwork (Thomas, 1949; Eaton, 1980; Lang and Eastoe, 1988).

The vein deposits typically consist of bands of quartz-sulfide material with fault gouge, with crustiform and other open-space-filling textures common. Lang and Eastoe (1988) describe the paragenetic sequence of the polymetallic quartz veins in detail, but in brief, the initial mineralization is strong silicification with minor pyrite, followed by brecciation and crustiform quartz + sericite with either pyrite + arsenopyrite or sphalerite + galena, and then by a quartz + carbonate + chalcopyrite + pyrite. A final supergene phase occurs that is dependent on the vein mineralogy. Alteration associated with the polymetallic veins is not well-described due to the lack of fresh exposures, but historic descriptions from Thomas (1949) and summarized by Lang and Eastoe (1988) from some of the historic underground workings suggest strong silicification near the veins to intense quartz + sericite + pyrite that weakens with distance, and a later argillic overprint proximal to the vein.

Lang and Eastoe (1988) interpret the polymetallic quartz veins as not directly related to the porphyry mineralization event, but instead to be penecontemporaneous to the Cretaceous magmatism.

Exotic copper mineralization

The Emerald Isle mine, located about 2 miles west of the Mineral Park mining complex, is a historic copper mine that first began producing in 1917 (Dings, 1951). From 1917-1993, Emerald Isle produced some approximately 23,400,900 lbs of copper from approximately 1.6 million tons of mineralized material (Table 2). The deposit has an NI 43-101-compliant resource of 2.22 million tons of 0.62% Total Copper, accounting for approximately 27.5 million pounds of copper (Agnerian and Postle, 2006).

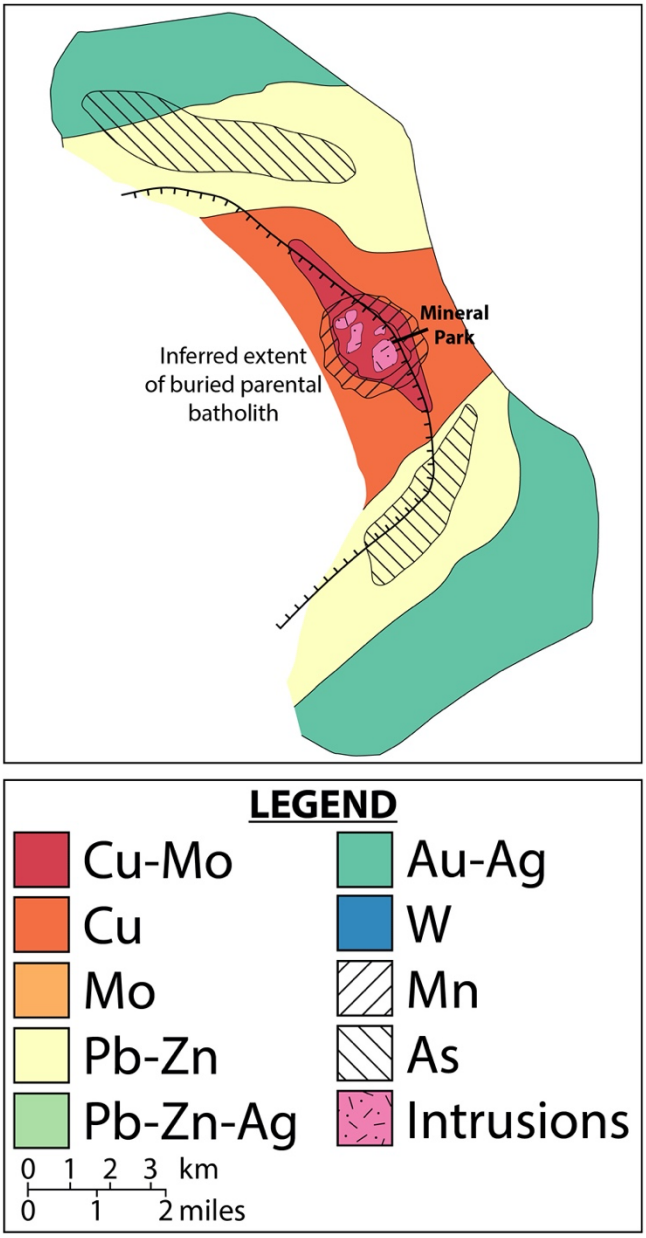

Figure 4. Metal zoning in the Wallapai district (after Lang and Eastoe, 1988).

The Emerald Isle copper deposit is principally hosted within a polymict conglomerate (map unit QTcg) that some previous workers have refered to as the "Gila Conglomerate". Mineralization primarily consists of bluish-green chrysocolla, with tenorite/copper pitch, malachite, manganese oxide, and rare cuprite and dioptase (D'Andrea et al., 1977; Agnerian and Postle, 2006). A subvertical N30°E-striking fissure vein with the same ore mineralogy as the conglomerate-hosted mineralized was noted in the early production of the mine (Thomas, 1949). Mineralization forms much of the matrix between clasts within the conglomerate, and while predominantly within the conglomerate, mineralization can extend into the overlying surficial deposits and underlying crystalline rocks. Clasts compositions include Proterozoic igneous and metamorphic rocks, Cretaceous porphyritic rocks, and rare volcanic clasts. While no volcanic rocks were mapped in the Cerbat quadrangle, in the surrounding quadrangles, abundant Miocene volcanic rocks are present (Varga, 2001; Ferguson et al., 2009; Johnson et al., 2022).

Table 2. Emerald Isle Production History

Period	Mineralized Material (Tons)	Mineralized Material (lbs)	Copper (lbs)	Notes	Reference
1917-1974	1,418,000	2,836,000,000	22,166,000	400 oz of silver and an indeterminate amount of gold were also produced during this interval.	Keith et al. (1986)
1987(?)	50?	100,300	82,246	Exact time frame is uncertain.	Agnerian and Postle (2006)
July 1992-September 1993	179,197	358,394,000	1,152,663	Exact figures for production during this period vary, but estimates all within the same order of mangitude	Agnerian and Postle (2006)
Totals	**1,597,247**	**3,194,494,300**	**23,400,909**	-	-

While the exact age of the mineralization is unknown, the presence of rare (likely Miocene) volcanic clasts within the conglomerate precludes it being older than Miocene, and the extension of the mineralization into the surficial deposits allows the timing of mineralization to be relatively recent. The source of the copper is not definitively known either. The sizable Mineral Park mining complex is proximal and presents one possibility, but the drainages dominantly lead away from Emerald Isle. The weakly mineralized porphyry copper occurrence at Alum Wash has been suggested as a potential source as several of the modern drainages that come off the Alum Wash prospect passing through the Emerald Isle mine area (Agnerian and Postle, 2006) Drilling beyond he pit boundaries has partially constrained the lateral extent of the conglomerate within a paleochannel that may have been sourced from Alum Wash, but details on the geometry, orientation, and location of drill holes defining the paleochannel are lacking. A conglomerate cemented by iron oxides and minor manganese and copper oxides is described by Vega (1984) and may be correlative with the conglomerate at the Emerald Isle mine.

Recent workers (e.g., Agnerian and Postle, 2006; Price, 2015) have described a small silicified intrusive body. Price (2015) suggests that there is a poorly recognized porphyry stock directly underlies the Emerald Isle pit. This is based on reinterpretation of the final lithologic units and descriptions encountered in historic El Paso Natural Gas Company drill holes by Price (2015), with reference to specific intervals of "long sections of mineralized porphyry" in drill holes A-2 and A-3. Reexamination of the original El Paso Natural Gas Company drill logs (available at https://minedata.azgs.arizona.edu/report/emerald-isle-0) by the lead author reveal common rock types encountered below QTcg in the referenced intervals include "granite gneiss" and "granite" with generally poorly described, but variably intense, hydrothermal alteration (AZGS Mining Data, 2014). While the consistent mention of hydrothermal alteration within the

bedrock geology of the holes raises questions, the lack of detailed lithologic descriptions within the available drill logs or examination of the original drill core prevents full evaluation of the suggestion that there could be a proximal, buried porphyry system near Emerald Isle.

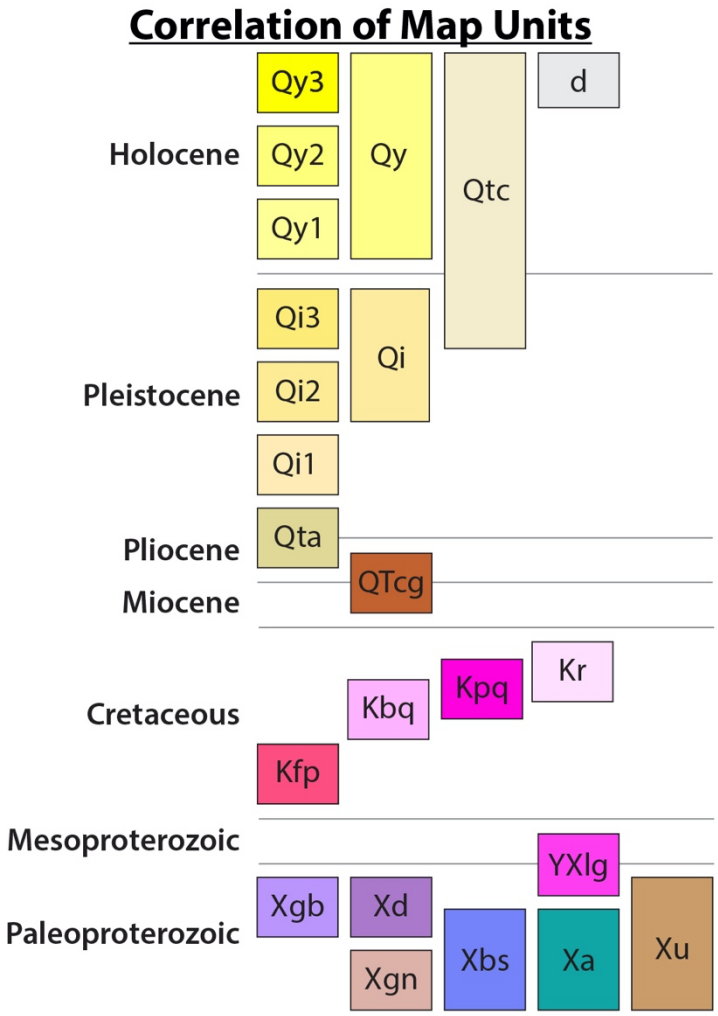

Figure 5. *Correlation of map units showing the chronologic relations between map units in the Cerbat 7.5' quadrangle.*

UNIT DESCRIPTIONS

The correlation of map units (Fig. 5) depicts the chronological relations between map units in the study area.

Quaternary

Qu – Surficial and basin deposits, undivided (Quaternary to Pliocene): Undivided surficial and basin deposits (cross section only).

Qy3 - Deposits in larger channels, gravel bars and adjacent low terraces (late Holocene): Very poorly sorted sand, pebbles, and cobbles, with minor silt and clay; boulders are common closer to bedrock hills and mountains. Channel topography is flat to gently undulating; bars and terraces are less than 1m higher than adjacent channels; all are part of active fluvial systems. Clast lithologies are crystalline metamorphic and intrusive rocks, with minor mafic volcanics.

Qy2 – Young deposits in low terraces and expansion reaches (late Holocene): Very poorly sorted sand, pebble, cobble, boulder, and silt deposits in low terraces adjacent to active channels and broad flow expansion reaches. Topography typically undulates between channels, terraces, and gravel bars. Surface color is typically brown. Some open gravel surface lags, but no desert pavement or soil development.

Qy1 – Young deposits in low terraces and alluvial fans (Holocene): Very poorly sorted sand, pebble, cobble, boulder, and silt deposits in low terraces and portions of young alluvial fans that are farther from active channels and/or higher than nearby Qy2 surfaces. Qy1 surfaces typically are undulating with coarse gravel bars and relict channels but may be planar where deposits are fine-grained. Deposits in relict channels are generally fine-grained, but commonly are covered by fine open pebble to cobble lags. Gravel bars between relict channels are obvious but somewhat subdued. Surface color is typically brown to gray. Soil development is weak to moderate, with some soil structure and visible carbonate accumulations.

Qy - Undivided young alluvial deposits (Holocene).

Qi3 - Young intermediate age deposits in relict alluvial fans and terraces (late Pleistocene): Poorly sorted mixtures of silt, sand, pebbles, cobbles, with some boulders close to the mountains, found in inactive alluvial fans and stream terraces. Qi3 surfaces are typically 1-2m higher than nearby active channels. Surface topography varies from gently undulating relict bars and swales where deposits are coarse-grained to quite smooth where deposits are finer grained. Soil development is moderate, with some clay accumulation and reddening of surface soil. Carbonate coatings typically are thin and discontinuous. Qi3 deposits are of limited extent near the mountain front but more extensive in middle and lower piedmont areas.

Qi2 – Intermediate age deposits in relict alluvial fans (middle to late Pleistocene): Very poorly sorted sand, pebbles, cobbles, and boulders, with minor silt and clay. Soil development is moderate to strong, with reddened, clay-rich argillic horizons and obvious surface reddening; carbonate accumulations on gravel clasts and carbonate accumulation between clasts obvious. Rock varnish is variable, but typically is orange. Margins of relict fan surface remnants are well rounded. Qi2 deposits are predominant in upper and middle piedmont areas.

Qi - Undivided intermediate alluvial fan and terrace deposits, including Qi2 or Qi3 deposits (middle or late Pleistocene).

Qi1 – Older intermediate deposits in eroded relict alluvial fans (middle Pleistocene): Very poorly sorted sand, pebbles, cobbles, silt, clay, and boulders found in moderately to deeply eroded alluvial fans. Planar alluvial fan surface remnants are limited in extent; much of this unit consists of eroded slopes formed on alluvial fan deposits. Well-preserved planar surfaces are

slightly reddened (orange), but more eroded areas commonly are light in color. Carbonate soil development is variable, but generally is strong; thin laminar petrocalcic horizons (weak stage IV) are exposed in roadcuts and on the slopes formed on these deposits. Qi1 deposits are less extensive than Qi2 and Qi3 deposits and are found only in middle and upper piedmont areas.

QTa – Old coarse alluvial fan deposits (early Pleistocene to Pliocene): Poorly sorted cobbles, pebbles, boulders, and sand with minor silt. Surfaces consist of rounded ridges and small valleys, with several meters or more of local topographic relief. Soil development is moderate to weak. QTa deposits are only exposed near the mountains, where they are substantially higher in the landscape than any younger deposits.

Qtc – Hillslope colluvium and talus (Quaternary): Very poorly sorted, angular to subangular, locally derived gravel, sand, silt, and clay deposits derived from immediately adjacent bedrock. Material is derived from underlying or adjacent bedrock outcrops. Locally includes very limited cobble-boulder talus deposits and areas of weathered bedrock where there are no outcrops.

QTcg – Conglomerate (Miocene to Quaternary): Generally well-cemented, polymict conglomerate with sand to cobble-sized clasts, and locally boulder-sized (up to 4 feet) clasts (Dings, 1951). Clasts are commonly angular to subangular, with lesser rounded clasts, and composed of Cretaceous porphyritic rocks, Proterozoic igneous and metamorphic rocks, and rare volcanic clasts (AZGS Mining Data Files, 2014). The conglomerate is well mineralized and was first mined as the Emerald Isle mine in the late 1910's (Dings, 1951). Mineralization consists of bluish-green chrysocolla, with tenorite/copper pitch, malachite, manganese oxide, and rare cuprite and dioptase (D'Andrea et al., 1977; Agnerian and Postle, 2006). Drilling around the Emerald Isle open pit has partially constrained the extent of the conglomerate, with the suggestion by past workers (e.g., Agnerian and Postle, 2006) that the unit is confined to a paleochannel that was sourced from the Alum Wash area along the Cerbat-Chloride 7.5' quadrangle boundary. A poorly mineralized conglomerate cemented by iron oxides and minor manganese and copper oxides is documented by Vega (1984) at Alum Wash and may be correlative to QTcg.

d - Areas substantially altered by human activities, primarily major roadways and mining areas (late Holocene).

Cretaceous

Kr - Rhyolite: White to buff to light pink rhyolite dikes are present throughout the map area, where they have a dominant northwest-southeast strike and a subordinant north/northeast to south/southwest strike. The dikes are aphanitic to microcrystalline with 1-2% K-feldspar phenocrysts and rare rounded quartz phenocrysts. The groundmass is 60% K-feldspar and 40% quartz, with accessary apatite and zircon. The dikes typically have sharp contacts and exhibit flow banding along the dike margins. The rhyolite dikes are mappable as far south as ~1 km from the southern boundary of the Cerbat quadrangle, and continue as far north as Chloride. The spatial coincidence with the distribution of the vein mineralization, all centered along the Ithaca Peak stock, suggests they are genetically related to the same underlying magmatic source (Lang and Eastoe, 1988).

Age relations for the rhyolite dikes and the Ithaca Peak quartz monzonite are from previous workers interpreting rhyolite dikes to cut rocks in the western part of the Mineral Park mine complex that were interpreted to be quartz monzonite porphyry (e.g., Eidel et al, 1968; Wilkinson et al., 1982). However, Vega (1984) suggests that given the known difficulties in distinguishing altered quartz monzonite porphyry and quartz-feldspar gneiss (herein lumped into Xu given the variation in the Proterozoic geologic units observed elsewhere in the Cerbat quadrangle), that this age relation may not be correct. A recent attempt at U-Pb zircon geochronology of a rhyolite dike collected near Mineral Park failed due to the thinness of the Cretaceous rims of the zircon grains compared to the width of the laser (Greig, 2022).

Ithaca Peak quartz monzonite: The Ithaca Peak quartz monzonite consists of six stocks at the Mineral Park mine, of which at least 5 are partially exposed at the present surface. The largest of the stocks, the Ithaca Peak stock at Ithaca Peak, is a composite stock of outer biotite quartz monzonite porphyry and inner aplitic quartz porphyry. The other stocks are all predominantly biotite quartz monzonite porphyry. Descriptions of earlier mapping of the range by Dings (1951) noted several additional occurrences of "Ithaca Peak granite," which have been previously reinterpreted as intensely hydrolytically-altered Proterozoic rocks by Loghry and Heinrichs (1980) and confirmed in this study.

Cretaceous intrusive and host rocks in the mine area are hydrothermally altered, with secondary biotite interpreted as the oldest and most widespread alteration product. Igneous biotite in the Cretaceous igneous rocks and gneissic host rocks is typically partially recrystallized with the addition of rutile, and the replacement of hornblende in the amphibolite (Xa) and diorite (Xd) by biotite + quartz + magnetite (+ carbonate in amphibolite). Less abundant, but relatively widespread, hydrothermal occurrences of K-feldspar rims on plagioclase and partial to complete replacement of plagioclase are present. Detailed descriptions of the veinlet-controlled alteration-mineralization is provided by Wilkinson et al. (1982).

Kqp - Quartz porphyry: Fine-grained, porphyritic-aplitic quartz monzonite porphyry, with 10% large (≤1.5 cm) rounded and embayed quartz "eyes," 20% plagioclase, 3% biotite, and occasional (~2%) large (≥ 4 cm) K-feldspar phenocrysts in an aplitic groundmass. Near the center of the quartz porphyry is an elliptical zone of crenulated, sinuous quartz veins and pods with unidirectional solidification textures (USTs).

Kbp - Biotite quartz monzonite porphyry: Medium-grained, porphyritic-phaneritic to porphyritic-aphanitic quartz monzonite porphyry to lesser quartz diorite porphyry (only identifiable via petrography according to Wilkinson et al., 1982). Euhedral to subhedral phenocrysts of 35-50% plagioclase, 2-10% biotite, 4-5% quartz, up to 2% K-feldspar, and accessory apatite, rutile, and zircon. An intermediate phase of quartz monzonite porphyry (not shown) is mapped at the mine located between the biotite quartz monzonite porphyry and quartz porphyry (Kqp); however, the unit is only distinguishable from the biotite quartz monzonite porphyry by the sericitization of biotite. The vertical extent of sericitization coincides with the chalcocite enrichment blanket, suggesting the quartz monzonite porphyry is not a separate rock type, but a supergene alteration product (Wilkinson et al., 1982). A U-Pb zircon weighted mean age of 73.2 ± 0.5 Ma was obtained from a sample of the border phase of the Ithaca Peak stock (Greig, 2021).

Kfp - Feldspar porphyry dike: Weakly to moderately porphyritic with 20-25% plagioclase, 3-15% quartz (rarely in the form of quartz eyes), 5% mafic minerals (intense alteration precludes confident identification, but shapes of altered mafic mineral sites in thin section suggest biotite and amphibole), and 2-5% K-feldspar. Intensely hydrolytically altered (individual feldspar grains up to 60% replaced by sericite in thin section) with sericite dominantly the groundmass. Hematite also present in thin section, likely as a weathering product of an earlier iron-oxide. Magnetite is present in samples collected near near the Little Ithaca area.

The Bronco dike, from which sample CAR-CB20-29 was collected, were formerly mapped as a Laramide felsite dike by Dings (1951) and interpreted to emanate from a mass of "Ithaca Peak granite" to the southeast of the tailings pile. Dikes, such as the Bronco dike, were reinterpreted as altered dacite dikes by Loghry and Heinrichs (1980). These may also be analogous to the porphyritic quartz latite and latite porphyry described by Vega (1984). A U-Pb zircon weighted mean age of 74.5 ± 0.7 Ma was obtained from CAR-CB20-29.

Mesoproterozoic to Paleoproterozoic

YXlg - Leucogranite and pegmatite: Aplitic to coarse-grained leucogranite and pegmatite dikes, commonly occurring within and along the margins of other metamorphic rocks. There are likely multiple generations of Paleoproterozoic leucogranites and pegmatite dikes, with clear evidence that at least some leucogranites must have intruded the amphibolite and biotite schist bodies prior to folding. Ptygmatic folds are common of YXlg are common in the more intensely migmatized areas of granite and gneiss (map unit Xgn). Leucogranite dikes clearly cut the northeast-striking, subvertical foliation in some locations with one sample, CAR-20CB-09B, collected from one such location. Results from U-Pb zircon geochronology yielded LA-ICP-MS dates ranging from 2670 ± 20 to 1431 ± 37 Ma. The three youngest dates yield a weighted mean of 1439 ± 26 Ma and is interpreted to be the crystallization age.

Paleoproterozoic

Xgb - Gabbro: Fine- to medium-grained gabbro, greenish-black when fresh, reddish to dark brown when weathered. Medium-grained samples can have a distinct diabasic texture due to the presence of needle-like crystals of feldspars (25%) with interstitial pyroxene (45%) and olivine (30%). Olivine grains typically have alteration rims of serpentinite and/or chlorite in thin section. Accessory minerals include magnetite, calcite, and apatite.

Xd - Diorite: Medium- to coarse-grained, aphanitic to weakly porphyritic diorite with 25-50% plagioclase, 25-35% quartz, 10-15% hornblende (typically replaced by hydrothermal biotite near the Mineral Park mine), 5-15% igneous biotite, and 0-20% K-feldspar. The occurrences distal to the Mineral Park mining complex contain intact igneous hornblende.

Xu - Undifferentiated metamorphic and plutonic rocks: Undivided metamorphic and plutonic rocks, including amphibolite, biotite schist, diorite, gabbro, undivided gneisses and granite. Units large enough to be mappable are separated out as distinct bodies, while much of the unit consists of finely interfoliated mixtures of the constituent units.

Xgn - Granite and gneiss: Variably foliated fine to medium-grained granitic to quartz monzonitic orthogneiss. Granitic rocks contain 5-10% biotite. Ptygmatic folds of leucogranite and pegmatite (map unit YXlg) are common in more intensely migmatized zones. Banding in the gneiss is defined by biotite-rich melanosomes ranging in thickness from 1 cm to 2 m. Lueucosomes contain locally abundant (up to 10%) zones of 1-3 mm garnets. The contact with Xu is generally gradational, with an increase in inclusions of other rock types towards the contact. Duebendorfer et al. (2001) documented a magmatic garnet-biotite schist and paragneiss (also containing sillimanite and cordierite) elsewhere in the Cerbat Mountains, allowing for some of the northern Xgn along the contact to have a possible metasedimentary origin.

Xam - Amphibolite: Fine-grained amphibolite characterized by alternating hornblende-rich black layers and diopside-plagioclase brown-weathered layers. The diopsidic layers range from 1.5-6 cm thick. Thin amphibolite layers (1-2 meters) can be found throughout the map area, to a few hundred meters. Hornblende laths are best exposed on weather surfaces, typically only a few mm long, but can be as long as 5-7 mm. The largest occurrence of amphibolite is spatially coincident with the Ithaca Peak stocks at the Mineral Park mining complex.

Whole-rock geochemical analysis of nine occurrences of amphibolite near the town of Chloride found minimal spread in data, suggesting the amphibolite bodies there were all derived from a single lithologic unit (Eaton, 1980). In a corral in Big Wash, 4.5 km northwest of Chloride, amphibolites are observed to have relict pillow structures and alteration rinds (Duebendorfer et al., 1998). Given the proximity between the Big Wash corral and Chloride, all of the amphibolites to the north of the Cerbat quadrangle may likely be metavolcanic in origin. This may apply to the amphibolites of Cerbat and Stockton Hill; however, without more definitive evidence such as relict pillow structures and alteration rinds within the Cerbat and Stockton Hill quadrangles this remains conjecture.

Xbs - Biotite schist: Fine- to medium-grained, strongly-foliated schist with 40-60% biotite, 10-50% plagioclase, 10-30% quartz, and accessory apatite, magnetite, and titanite. Individual biotite grains are often platy and can be as large as 5-10 mm.

References

Agnerian, H., and Postle, J. T., 2006, NI 43-101 technical report on the Emerald Isle copper deposit, Arizona, U.S.A., prepared for Ste. Genevieve Resources, Ltd., 10 March 2006, 95 p.

Atkinson, W. W., and Ware, H. W., 2002, Comb quartz layers in the porphyry copper deposit at Yerington, Nevada [abs]: Geological Society of America Abstracts with Programs, v. 34, no. 5, p. A-15.

AZGS Mining Files Data, 2014, Emerald Isle Heinrichs GEOEXploration Item 1994-01-0108B, Grover Heinrichs mining collections, Arizona Geological Survey (https://minedata.azgs.arizona.edu/report/emerald-isle-0, accessed 17 January 2022).

Beard, L. S., and Faulds, J. E., 2011, Kingman uplift, paleovalleys, and extensional foundering in northwest Arizona, in Beard, L. S., Karlstrom, K. E., Young, R. A., and Billingsley, G. H., eds., CRevoltuion 2 - Origin and evolution of the Colorado River system, workshop abstracts: U.S. Geological Survey Open-File Report 2011-1210, p. 28-37.

Bull, W. B., 1991, Geomorphic Responses to Climate Change: Oxford University Press, 352 p..

D'Andrea, D. V., Larson, W. C., Fletcher, L. R., Chamberlain, P. G., and Engelmann, W. H., 1977, In situ leaching research in a copper deposit at the Emerald Isle mine: Bureau of Mines Report of Investigations 8236, 43 p.

Drake, W. E., 1972, A study of ore-forming fluids at hte Mineral Park porphyry copper deposit, Kingman, Arizona: Unpublished Ph.D. dissertation, Columbia University, New York City, 245 p.

Dings, M. G., 1951, The Wallapai mining district, Cerbat Mountains, Mohave County, Arizona: U.S. Geological Survey Bulletin 978-E, p. 123-163.

Donner, C., 1997, Diplomkartierung der Cerbat Mountains zwischen Pine und Antelope Canyon östlich von Dolan Springs, Arizona, USA: Unpublished M.S. thesis, Eberhard-Karls-Universität Tübingen, Tübingen, Germany, 21 p.

Duebendorfer, E. M., Nyman, M. W., Chamberlain, K. R., and Jones, C. S., 1998, Proterozoic rocks within the Mojave-Yavapai boundary zone, northwestern Arizona: Comparison of metamorphic and structural evolution across a major lithospheric(?) structure, in Duebendorfer, E. M., ed., Geologic excursions in northern and central Arizona: Field Trip Guidebook for Geological Society of America, Rocky Mountain Section Meeting, Northern Arizona University, Flagstaff, p. 127-148.

Duebendorfer, E. M., Chamberlain, K. R., and Jones, C. S., 2001, Paleoproterozoic tectonic history of the Cerbat Mountains, northwestern Arizona: Implications for crustal assembly in the southwestern United States: Geological Society of America Bulletin, v. 113, p. 575-590.

Eaton, L. G., 1980, Geology of the Chloride mining district, Mohave County, Arizona: Unpublished M.S. thesis, New Mexico Institute of Mining and Technology, Socorro, 133 p. text, unpaginated appendices, and 1 plate.

Eidel, J. J., Frost, J. E., and Clippinger, D. M., 1968, Copper-molybdenum mineralization at Mineral Park, Mohave County, Arizona, *in* Ridge, J. D., ed., Ore deposits of the United States, 1933-1967, 2, New York, American Institute of Mining, Metallurgical, and Petroleum Engineers, p. 1258-1281.

Fitzgerald, P. G., Duebendorfer, E. M., Faulds, J. E., and O'Sullivan, P., 2009, South Virgin–White Hills detachment fault system of SE Nevada and NW Arizona: Applying apatite fission track thermochronology to constrain the tectonic evolution of a major continental detachment fault: Tectonics, v. 28.

Faulds, J. E., Schrieber, B. C., Reynolds, S. J., Okaya, D., and Gonzalez, L., 1997, Origin and paleogeography of an immense, nonmarine Miocene salt deposit in the Basin and Range (western U.S.A.): Journal of Geology, v. 105, p. 19-36.

Faulds, J. E., Feuerbach, D. L., Miller, C. F., and Smith, E. I., 2001, Cenozoic evolution of the northern Colorado River extensional corridor, southern Nevada and northwest Arizona, in Erksine, M. C., Faulds, J. E., Bartley, J. M., and Rowley, P. D., eds., The Geologic Transition, High Plateaus to Great Basin - A Symposium Field Guide: The Mackin Volume, Utah Geological Association, Publication 30, p. 239-271.

Ferguson, C. A., and Cook, J. P., 2015, Geologic map of the Kingman 7.5' Quadrangle, Mohave County, Arizona: Arizona Geological Survey Digital Geologic Map 113, scale 1:24,000.

Ferguson, C. A., Johnson, B. J., Pearthree, P. A., and Spencer, J. E., 2009, Geologic map of the Grasshopper Junction 7.5' Quadrangle, Mohave County, Arizona: Arizona Geological Survey Digital Geologic Map 70, scale 1:24,000, 2 plates.

Greig, R. E., 2021, Superposed magmatic and hydrothermal systems, and the evolution of the Laramide arc and porphyry copper province, southwestern North America: Unpublished Ph.D. dissertation, University of Arizona, Tucson, 346 p.

Hanlon, J. D., 1997, Structure and petrology of Proterozoic rocks in the Tennessee Wash area, Cerbat Mountains, northwestern Arizona: Unpublished M.S. thesis, Northern Arizona University, Flagstaff, 115 p. and 2 plates.

Heidrick, T. L., and Titley, S. R., 1982, Fracture and dike patterns in Laramide plutons and their structural and tectonic implications, in Titley, S. R., ed., Advances in geology of the porphyry copper deposits, southwestern North America: Tucson, University of Arizona Press, p. 73-90.

Henrik, S., 1998, Geologische Kartierung nördlich von Klingman (S-Cerbat Mountains, Arizona, USA): Unpublished M.S. thesis, Eberhard-Karls-Universität Tübingen, Tübingen, Germany, 47 p.

Johnson, B. J., Pearthree, P. A., Richardson, C. A., and Ferguson, C. A., 2022, Geologic map of the Stockton Hill 7.5' quadrangle, Mohave County, Arizona: Arizona Geological Survey Digital Geological Map DGM-152, scale 1:24,000, 2 sheets, and text.

Jones, C. S., 1998, Proterozoic geologic history of the Vock Canyon area, Cerbat Mountains, northwestern Arizona: Unpublished M.S. thesis, Northern Arizona University, Flagstaff, 125 p. and 2 plates.

Keith, S. B., Gest, D. E., DeWitt, E., Troll, N. W., and Everson, B. A., 1986, Metallic mineral districts and production in Arizona: Arizona Bureau of Geology and Mineral Technology Bulletin 194, 62 p.

Kirwin, D., 2006, Unidirectional solidification textures, miarolitic cavities and orbicles: Field evidence for the magmatic to hydrothermal transition in intrusion-related mineral deposits: Proceedings of the 19th General Meeting of the International Mineralogical Association, v. 185.

Kollet, S., 1998, Diplomkartierung der Cerbat Kingman/Arizona (USA): Unpublished M.S. thesis, Eberhard-Karls-Universität Tübingen, Tübingen, Germany, 28 p.

Laine, R. P., 1974, Geological-geochemical relationships between porphyry copper and porphyry molybdenum ore depostis: Unpublished Ph.D. dissertation, University of Arizona, Tucson, 326 p.

Lang, J. R., 1986, A geochemical study of alteration and mineralization in the Wallapai mining district, Mohave County, Arizona: Unpublished M.S. thesis, University of Arizona, Tucson, 142 p.

Lang, J. R., and Eastoe, C. J., 1988, Relationships between a porphyry Cu-Mo deposit, base and precious metal veins, and Laramide intrusions, Mineral Park, Arizona: Economic Geology, v. 83, p. 551-567.

Lang, J. R., Guan, Y., and Eastoe, C. J., 1989, Stable isotope studies of sulfates and sulfides in the Mineral Park porphyry Cu-Mo system, Arizona: Economic Geology, v. 84, p. 650-662.

Lee, W. T., 1908, Geologic reconnaissance of a part of western Arizona: U. S. Geological Survey Bulletin 395, 96 p.

Loghry, J. D., and Heinrichs, W. E., Jr., 1980, Geologic evaluation of uranium in plutonic rocks, northwestern Arizona: U.S. Department of Energy Report GJBX-213(80), 214 p.

Lowenstern, J. B., and Sinclair, W. D., 1996, Exsolved magmatic fluid and its role in the formation of comb-layered quartz at the Cretaceous Logtung W-Mo deposit, Yukon Territory, Canada: Transactions of The Royal Society of Edinburgh, v. 87, p. 291-303.

Lucchitta, I., 1975, The Shivwits Plateau, in Goetz, A. F. H., Billingsley, G. H., Gillespie, A. R., Abrams, M. J., Squires, R. L., Shoemaker, E. M., Lucchitta, I., and Elston, D. P., eds., Application of ERTS images and image processing to regional geologic problems and geologic mapping in northern Arizona: Jet Propulsion Laboratory Technical Report 32-1597, p. 41-73.Malmon, D. V., Howard, K. A., House, P. K., Lundstrom, S. C., Pearthree, P. A., Sarna-Wojcicki, A. M., Wan, E., and Wahl, D.B., 2011, Stratigraphy and depositional environments of the upper Pleistocene Chemehuevi Formation along the lower Colorado River: U.S. Geological Survey Professional Paper 1786, 95 p.

Murray, K. E., Braun, J., and Reiners, P. W., 2018, Toward robust interpretation of low-temperature thermochronometers in magmatic terranes: Geochemistry, Geophysics, Geosystems, v. 19, p. 3739-3763.

Mörz, T., 1996a, Petrographische und geochemische Untersuchungen an granitoiden Gesteinen in den Cerbat Mountains, Arizona: Unpublished M.S. thesis, Eberhard-Karls-Universität Tübingen, Tübingen, Germany, 80 p.

Mörz, T., 1996b, Der Proterozoische Cerbat Mountain Complex in NW-Arizona (USA), als möglicher Teil der Mojave/Yavapai-Sutur: eine petrographische und strukturelle Aufnahme: Unpublished M.S. thesis, Eberhard-Karls-Universität Tübingen, Tübingen, Germany, 198 p.

Orr, T. R., 1997, Proterozoic geology of the northern Cerbat Mountains: Implications for the evolution of the Mojave/Yavapai crustal boundary zone: Unpublished M.S. thesis, Northern Arizona University, Flagstaff, 90 p., and 1 plate.

Palais, D. G., 1991, Field, analytical, and theoretical studies of low pressure metamorphism in Arizona: Unpublished Ph.D. dissertation, Arizona State University, Tempe, 183 p.

Price, B. J., 2015, Emerald Copper Oxide Project: technical report prepared for Napier Ventures, Inc., 22 December 2015, 83 p.

Richard, S. M., Reynolds, S. J., Spencer, J. E., and Pearthree, P. A., 2000, Geologic Map of Arizona: Arizona Geological Survey Map 35, 1:1,000,000 scale.

Schneider, J., 1997, Petrographie und Geochemie im Proterozoikum und Tertiär der nördlichen Cerbat Mountains, Arizona, USA: Unpublished M.S. thesis, Eberhard-Karls-Universität Tübingen, Tübingen, Germany, 89 p.

Schrader, F. C., 1909, Mineral deposits of the Cerbat Range, Black Mountains, and Grand Wash Cliffs, Mohave County, Arizona: U. S. Geological Survey Bulletin 397, 226 p.

Seedorff, E., Dilles, J. H., Proffett, J. M., Jr., Einaudi, M. T., Zurcher, L., Stavast, W. J. A., Johnson, D. A., and Barton, M. D., 2005, Porphyry deposits: Characteristics and origin of hypogene features, in Hedenquist, J. W., Thompson, J. F. H., Goldfarb, R. J., and Richards, J. P., eds., Economic Geology 100th Anniversary Volume, p. 251-298.

Shannon, J. R., Walker, B. M., Carten, R. B., and Geraghty, E. P., 1982, Unidirectional solidification textures and their significance in determining relative ages of intrusions at the Henderson Mine, Colorado: Geology, v. 10, p. 293-297.

Thomas, B. E., 1949, Ore deposits of the Wallapai district, Arizona: Economic Geology, v. 44, p. 663-705.

Thomas, B. E., 1953, Geology of the Chloride quadrangle, Arizona: Geological Society of America Bulletin, v. 64, p. 391-420, and 1 plate.

Varga, R. J., 2001, Geologic map of the Grasshopper Junction SE 7.5' quadrangle, Mohave County, Arizona: Arizona Geological Survey Contributed Map CM-04-B, map scale 1:24,000.

Vega, L. A., 1984, The alteration and mineralization of the Alum Wash prospect, Mohave County, Arizona: Unpublished M.S. thesis, University of Arizona, Tucson, 57 p. and 4 plates.

Vega, L. A., and Wilkinson, W. H., 1984, Visitor's Information Pamphlet - Duval Corporation, Mineral Park Property, in Wolfhard, M. R., Wilkins, J., Jr., Huskinson, E., Jr., Durning, P., Bonelli, D., Vega, L. A., and Wilkinson, W. H., eds., Structure and mineralization, Kingman area, Arizona: Arizona Geological Society Fall Field Trip Guidebook, unpaginated pages.

Wilkinson, W. H., 1981, The distribution of alteration and mineralization assemblages of the Mineral Park mine, Mohave County, Arizona: Unpublished Ph.D. dissertation, University of Arizona, Tucson, 101 p., and 5 plates.

Wilkinson, W.H. Jr., Vega, L.A., and Titley, S.R., 1982, Geology and Ore Deposits at Mineral Park, Mohave County, Arizona, in Titley S.R., ed., Advances in geology of the porphyry copper deposits, southwestern North America: Tucson, University of Arizona Press, p. 523-541.

Young, R. A., 1979, Laramide deformation, erosion and plutonism along the southwestern margin of the Colorado Plateau: Tectonophysics, v. 61, p. 25-47.

Young, R. A., 2001, Geomorphic, structural, and stratigraphic evidence for Laramide uplift of the southwestern Colorado Plateau margin in northwestern Arizona, in Erskine, M. C., Faulds, J. E., Bartley, J. M., and Rowley, P. D., eds., The Geologic Transition, High Plateaus to Great Basin - A Symposium Field Guide: The Mackin Valume, Utah Geological Association Publication 30, p. 227-237.